

Ferroelectric Hysteresis in Superconducting Bilayers

Yanfang Li,^{1,*} Xin-Zhi Li,^{1,*} and Wen-Yu He^{1,†}

¹State Key Laboratory of Quantum Functional Materials,
School of Physical Science and Technology, ShanghaiTech University, Shanghai 201210, China
(Dated: December 5, 2025)

Recently, coexisting ferroelectricity and superconductivity were reported in bilayer T_d - MoTe_2 and twisted bilayer graphene. Importantly, it was observed that an applied displacement field switches the superconductivity with a ferroelectric hysteresis. Such direct coupling between the ferroelectricity and superconductivity offers promising pathways for developing low-power, non-volatile memory devices. However, the coupling mechanism between the ferroelectricity and superconductivity remains poorly understood. In this work, we demonstrate that in a superconducting bilayer, the hysteretic switching of superconductivity can arise from an interlayer pairing. By deriving the Landau Ginzburg free energy expansion for the interlayer pairing, we show that along the ferroelectric hysteresis loop, the hysteretic exceeding of the critical polarization P_c that destroys the interlayer pairing leads to the hysteretic switching of superconductivity. The condition to have a ferroelectric hysteretic superconducting state is established to be $P_r < P_c < P_s$, where P_r and P_s denote the remanent and saturated polarization, respectively. Crucially, our scenario of interlayer pairing yields two predictions: (1) an enhancement of the upper critical displacement field with stronger interlayer coupling and (2) a pronounced, gate-tunable interlayer crossed Andreev reflection, both of which provide clear pathways for experimental verification.

Introduction.— Atomically thin two-dimensional (2D) ferroelectrics are appealing for next-generation non-volatile memories [1–3] and have generated significant scientific interest [4–11]. Recently, a number of 2D van der Waals layered materials have been found to exhibit ferroelectricity [10–33]. In these 2D ferroelectric materials, stacking configurations break the inversion symmetry and lead to electrically switchable polarizations [10, 11]. Remarkably, the hallmark of the ferroelectric order in these 2D materials is an electric polarization hysteresis loop under an out-of-plane displacement field [10–15, 34, 35].

For ferroelectrics in 2D metals, the ferroelectric hysteresis of electric polarization is manifested as a resistance hysteresis during sweeps of gate voltage [16–21]. This gate induced hysteresis of resistance has been observed in bilayer T_d - MoTe_2 [31, 32], establishing bilayer T_d - MoTe_2 as a ferroelectric metal. Most strikingly, the ferroelectric hysteresis of resistance in bilayer T_d - MoTe_2 persists from the normal state into the superconducting state [31, 32]. Moreover, similar ferroelectric hysteresis has been independently observed in superconducting twisted bilayer graphene [33]. Together, these consistent observations across two distinct superconducting bilayer systems provide compelling evidence for a direct coupling between ferroelectricity and superconductivity.

This discovery of coupled ferroelectricity and superconductivity in bilayer T_d - MoTe_2 and twisted bilayer graphene profoundly challenges the long-standing paradigm that ferroelectricity and superconductivity are mutually exclusive [36–38]. As the conventional incompatibility between ferroelectricity and superconductivity no longer holds in these superconducting bilayers, a fundamental question arises: what is the microscopic mechanism behind the intriguing coupling between the ferro-

electricity and superconductivity there?

In this work, we show that interlayer pairing naturally leads to the ferroelectric hysteresis of resistance in superconducting bilayers, providing a viable mechanism for the coupling between ferroelectricity and superconductivity. Experimentally, the notable ferroelectric hysteresis between finite resistance state and superconducting state reveals a ferroelectric switching of superconductivity: the enhanced electric polarization from a sufficiently large gate voltage destroys superconductivity, whereas the superconducting state coexists with the remanent electric polarization (P_r) at zero displacement field. The interplay between ferroelectric order and superconducting pairing is most clearly demonstrated in bilayer T_d - MoTe_2 , where the superconducting critical temperature T_c exhibits a dramatic increase as the electric polarization approaches reversal [31]. As the electric polarization usually reduces before reversal, these observations consistently indicate that the out-of-plane electric polarization is detrimental to the pairing in the superconducting bilayer. Through free energy analysis, we find that the interlayer pairing shown in Fig. 1 (a) satisfies this condition that the out-of-plane polarization induces a pair-breaking effect, yielding a critical polarization P_c that completely suppresses superconductivity. Crucially, we point out that the ferroelectric hysteretic switching of superconductivity requires $P_r < P_c < P_s$, where P_s denotes the saturated ferroelectric polarization (Fig. 2 (b)).

In the following, we first elucidate the suppressive effect of out-of-plane electric polarization on the interlayer pairing. Second, we develop a Landau Ginzburg theory of coupled ferroelectric polarization and interlayer pairing, showing that the hysteretic switching of superconductivity occurs as the electric polarization hysteretically exceeds P_c (Fig. 2(b)). Finally, we discuss the physical im-

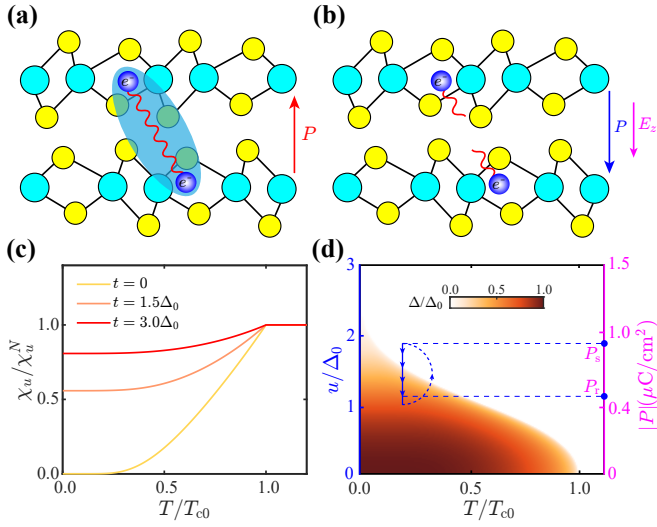


FIG. 1: Interplay between ferroelectric polarization and interlayer pairing. (a) At zero displacement field, the interlayer pairing coexists with the remanent electric polarization P_r in bilayer T_d -MoTe₂. (b) Upon switching, the reversed ferroelectric polarization exceeds the critical polarization P_c and abruptly destroys the interlayer pairing. (c) The electrostatic susceptibility χ_u in the superconducting regime with different interlayer couplings. Given $t \neq 0$, a finite χ_u at $T = 0$ K enhances u_c and stabilizes the interlayer pairing. (d) The u - T phase diagram. The right y axis shows the polarization P corresponding to a given u at $T = 0.2T_{c0}$. The blue trajectory in the diagram manifests the ferroelectric switching of superconductivity: under an external displacement field at $T = 0.2T_{c0}$, the polarization traces the ferroelectric hysteresis loop, and the hysteretic exceeding of P_c leads to the hysteretic switching of superconductivity. Here, T_{c0} denotes the critical temperature at $u = 0$. The interlayer coupling is set to be $t = 1.5\Delta_0$ with Δ_0 being the pairing order parameter at $T = 0$ and $u = 0$.

plications of interlayer pairing and propose experimental protocols to further test our scenario.

Interlayer pairing and out-of-plane polarization.— In a superconducting bilayer, the pair-breaking effect of out-of-plane electric polarization on the interlayer pairing is schematically illustrated in Fig. 1 (a) and (b). The interlayer pairing comprises Cooper pairs formed by electronic states from the top and bottom layers with opposite momenta $\pm \mathbf{k}$ (Fig. 1(a)). When a net out-of-plane electric polarization is present, the resulting electrostatic potential difference between the two layers [39] lifts the energy degeneracy of the electronic states forming interlayer Cooper pairs (Fig. 1(b)), thereby destabilizing the interlayer pairing. Above a critical polarization P_c , the saved electric polarization energy overcomes the interlayer pairing condensation energy, so superconductivity is completely suppressed by a mechanism analogous to the paramagnetic limiting in spin singlet superconductors [40, 41].

To quantitatively investigate the suppression of inter-

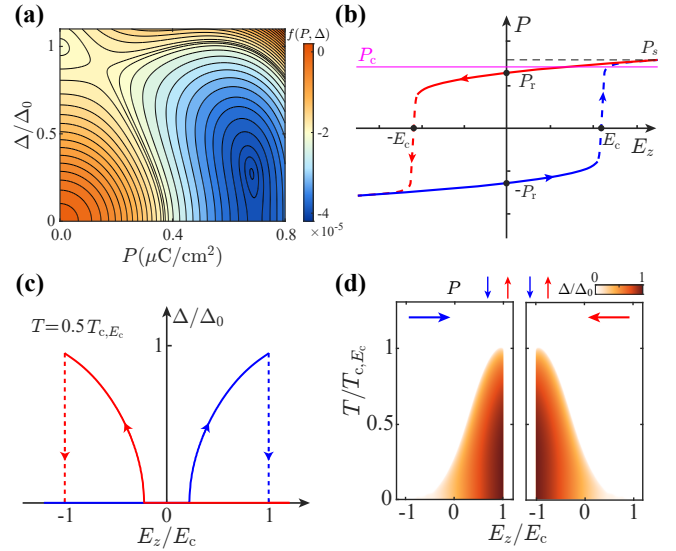


FIG. 2: Hysteretic coupling between ferroelectricity and superconductivity. (a) Contour plot of the free energy density $f(P, \Delta)$ at zero displacement field ($E_z = 0$). The global minimum of $f(P, \Delta)$ obtained at finite P and Δ confirms the coexistence of ferroelectricity and superconductivity. (b) The ferroelectric hysteresis loop of the polarization P under an external electric field E_z . The superconducting state, coexisting with the remanent polarization P_r at $E_z = 0$, is destroyed when P abruptly exceeds P_c at $|E_z| > E_c$. The corresponding hysteresis of the superconducting order parameter Δ . The switching of Δ between zero and a finite value directly manifests the resistance hysteresis that switches between finite and zero values. (d) Simulated temperature evolution of the coupled ferroelectricity and superconductivity. A dramatic increase in T_c is observed as the ferroelectric polarization approaches reversal (indicated by arrows on top). Here T_{c,E_c} denotes the critical temperature just prior to the polarization reversal.

layer pairing by out-of-plane electric polarization, we formulate an effective Bogoliubov-de Gennes (BdG) Hamiltonian matrix for the superconducting bilayer as [42]

$$H(\mathbf{k}) = \tau_z (\xi_{\mathbf{k}} \sigma_0 + u \sigma_z + t \sigma_x) s_0 + \Delta \tau_x \sigma_x s_0, \quad (1)$$

where τ_i , σ_i , and s_i ($i = 0, x, y, z$) are the identity and Pauli matrices in the Nambu space, layer space, and spin space respectively. The BdG Hamiltonian in Eq. 1 is in terms of the Nambu spinor $[c_{\mathbf{k},\sigma,s}^\dagger, -i s_{y,ss'} c_{-\mathbf{k},\sigma,s'}]$. Here $\xi_{\mathbf{k}}$ denotes the electronic band in the monolayer limit, u denotes the electrostatic potential energy manifesting a net out-of-plane electric polarization, t denotes the effective interlayer coupling, and Δ is the interlayer pairing order parameter. Given the absence of evidence connecting spin-orbit coupling to the ferroelectric switching of superconductivity, our superconducting bilayer model in Eq. 1 neglects effects of spin-orbit coupling and mainly focuses on the spin singlet pairing. We further show in the Supplementary Material [42] that spin-orbit coupling does not alter the essential physics of our model.

Employing the superconducting bilayer model in Eq. 1, we are able to quantify the competition between out-of-plane electric polarization and interlayer pairing to estimate the critical value of u that destroys superconductivity. In the normal state, the electric polarization energy is $\frac{1}{2}\chi_u^N u^2$. In the superconducting regime, the total saved energy, $-\frac{1}{2}N(0)\Delta^2 + \frac{1}{2}\chi_u u^2$, includes both the pairing condensation energy and the electric polarization energy of superconducting states. Here, χ_u^N and χ_u denote the electrostatic susceptibilities in the normal and superconducting states, respectively, and χ_u/χ_u^N is derived to take the form [42]

$$\frac{\chi_u}{\chi_u^N} = 1 - \pi k_b T \sum_n \frac{\Delta^2}{\sqrt{\omega_n^2 + \Delta^2} (\omega_n^2 + t^2 + \Delta^2)}, \quad (2)$$

with k_b being the Boltzmann constant and $\omega_n = (2n+1)\pi/(k_b T)$ denoting fermionic Matsubara frequency. By equating energies of the normal and superconducting states at zero temperature, we obtain the critical value of u at $T = 0$ K to be

$$u_c = \sqrt{N(0)/(\chi_u - \chi_u^N)}\Delta, \quad (3)$$

where $2N(0)$ is the density of states at Fermi level. In the limit of vanishing interlayer coupling $t = 0$, the electrostatic susceptibilities become $\chi_u = 0$ and $\chi_u^N = -2N(0)$, yielding $u_c = \Delta/\sqrt{2}$ that equals the Pauli paramagnetic limited Zeeman energy [40, 41]. In the more general case of finite interlayer coupling ($t \neq 0$), the electrostatic susceptibility χ_u acquires a finite value at $T = 0$ K (Fig. 1(c)), consequently enhancing u_c beyond $\Delta/\sqrt{2}$.

At finite temperature, u_c for the superconducting bilayer described by Eq. 1 can be further determined by minimizing the free energy density [42]

$$f = \frac{\Delta^2}{\bar{U}} + \sum_{\nu=\pm} \int_{\mathbf{k}} \left[(\xi_{\mathbf{k}}^\nu - E_{\mathbf{k}}^\nu) - \frac{2}{\beta} \log \left(1 + e^{-\beta E_{\mathbf{k}}^\nu} \right) \right] \quad (4)$$

with $\beta^{-1} = k_b T$, $\int_{\mathbf{k}} \equiv \int d\mathbf{k}/(2\pi)^d$, $\xi_{\mathbf{k}}^\pm = \xi_{\mathbf{k}} \pm \sqrt{u^2 + t^2}$, $E_{\mathbf{k}}^\pm = \sqrt{t^2 + u^2 + \Delta^2 + \xi_{\mathbf{k}}^2 \pm 2\sqrt{t^2 \xi_{\mathbf{k}}^2 + u^2 (\xi_{\mathbf{k}}^2 + \Delta^2)}}$ be-

ing the eigenvalues of $H(\mathbf{k})$ in Eq. 1, and \bar{U} denoting the effective interlayer pairing interaction in a unit cell. By minimizing Eq. 4 with respect to Δ , we obtain the u - T phase diagram shown in Fig. 1(d), where the phase boundary gives $u_c(T)$. It is noteworthy that only the interlayer pairing $\Delta\sigma_x$ gets continuously suppressed by the electrostatic potential energy u , while other pairings in the layer space do not exhibit this experimentally observed behavior [31, 42].

In the bilayer system described by Eq. 1, the electrostatic potential energy u is fundamentally connected to the out-of-plane electric polarization P through the relation [42]

$$P = edu \sum_{\nu=\pm} \int_{\mathbf{k}} \frac{1 - 2n(E_{\mathbf{k}}^\nu)}{2E_{\mathbf{k}}^\nu} \left[1 + \frac{4\nu (\xi_{\mathbf{k}}^2 + \Delta^2)}{(E_{\mathbf{k}}^+)^2 - (E_{\mathbf{k}}^-)^2} \right] \quad (5)$$

with $n(E_{\mathbf{k}}^\nu)$ being the Fermi Dirac distribution function, e denoting the elementary charge, and d being the distance between the two layers. At the phase boundary where the interlayer pairing vanishes, the critical polarization P_c that corresponds to u_c can be obtained via Eq. 5 by setting $\Delta = 0$. In the bilayer exhibiting spontaneous out-of-plane ferroelectric polarization, the finite electrostatic potential energy u is an intrinsic property of the system while remaining tunable via external gate voltage. Crucially, the u - T phase diagram in Fig. 1(d) along with Eq. 5 clearly demonstrates that interlayer pairing allows the coexistence of superconductivity with a moderate ferroelectric polarization, while polarization exceeding P_c destroys the superconducting state.

Landau Ginzburg theory of coupled ferroelectricity and superconductivity.— The above analysis has established that the superconducting state of interlayer pairing is compatible with a moderate out-of-plane ferroelectric polarization. However, the mechanism underlying the hysteretic switching of superconductivity requires further investigation. In the vicinity of phase transition, the phenomenological Landau Ginzburg free energy density incorporating both superconductivity and ferroelectricity is derived to take the form [42]

$$f(P, \Delta) = N(0) \left[\frac{T - T_{c0}}{T_{c0}} - g \left(\frac{\sqrt{u^2 + t^2}}{\pi k_b T} \right) \frac{2u^2}{u^2 + t^2} \right] \Delta^2 + \frac{1}{2} b_s \Delta^4 + a P^2 + \frac{1}{2} b P^4 - P \cdot E_z, \quad (6)$$

with $g(\rho) = \text{Re} \sum_{n=1}^{\infty} \left(\frac{1}{2n-1+i\rho} - \frac{1}{2n-1} \right)$, T_{c0} denoting the superconducting transition temperature at $u = 0$, and E_z denoting an external gate induced out-of-plane electric field. Here, the first two terms, obtained from the Taylor expansion of Eq. 4, describe the superconducting

state, while the last three terms govern the ferroelectric phase transition. The parameters b_s , a , and b respect $b_s > 0$, $a < 0$ and $b > 0$, where $a < 0$ guarantees a spontaneous ferroelectric polarization.

Notably, the coefficient of Δ^2 in Eq. 6 is seen to in-

volve the electrostatic potential energy u . Since u is fundamentally connected to P via Eq. 5, the ferroelectric polarization P directly affects the superconducting transition temperature, which reveals the intrinsic coupling between ferroelectricity and superconductivity. At zero displacement field ($E_z = 0$), combining Eq. 5 and Eq. 6 yields the density plot of $f(P, \Delta)$ shown in Fig. 2(a), where the global minimum of $f(P, \Delta)$ obtained at finite Δ and P manifests the coexisting interlayer pairing and ferroelectric polarization.

With the established Landau Ginzburg formalism in Eq. 6, we are now ready to elucidate the mechanism behind the hysteretic switching of superconductivity. It is known that in an external electric field, the ferroelectric order exhibits a hysteresis of polarization as schematically shown in Fig. 2(b). In the ferroelectric hysteresis curve, the spontaneous ferroelectric polarization at $E_z = 0$ is known to be the remanent electric polarization P_r . The coexistence of superconductivity with ferroelectricity requires the critical polarization P_c to satisfy $P_c > P_r$. Along the counterclockwise hysteresis path, as the applied electric field exceeds the coercive field E_c , the ferroelectric polarization reverses the direction and converges to the saturated polarization P_s . Crucially, in bilayer T_d -MoTe₂, it has been observed that the switching of superconductivity and the ferroelectric polarization reversal occurs simultaneously at the coercive field [31, 32], indicating that the critical polarization P_c respects $P_c < P_s$. Therefore, under the condition $P_r < P_c < P_s$, the hysteretic switching of superconductivity naturally arises from the polarization hysteretically exceeding P_c in the ferroelectric hysteresis loop (Fig. 1(d) and Fig. 2(b)).

Specifically, the Landau Ginzburg free energy density in Eq. 6 demonstrates that the ferroelectric hysteretic behavior in the superconducting state originates from three essential factors. First, the coupling between the ferroelectric order and external electric field generates a hysteresis of electric polarization. Second, the electric polarization modulates the superconducting transition temperature through the coefficient of Δ^2 in the free energy expansion. Third, the hysteretic switching of superconductivity is triggered by the condition $P_r < P_c < P_s$.

Guided by the established mechanism for the ferroelectric hysteretic superconducting state, we simulate the ferroelectric hysteresis of interlayer pairing via minimizing $f(P, \Delta)$ with respect to P and Δ across a range of applied electric fields E_z . Combining Eq. 5 and Eq. 6, we obtain both the hysteresis loop of pairing order parameter and the corresponding temperature evolution, shown in Fig. 2(c) and (d), respectively. Crucially, the pairing hysteresis from $\Delta = 0$ to finite Δ in Fig. 2(c) corresponds directly to the hysteresis between finite resistance and superconducting states observed in transport experiments. Remarkably, Fig. 2(d) captures the dramatic enhancement of T_c as ferroelectric polarization approaches

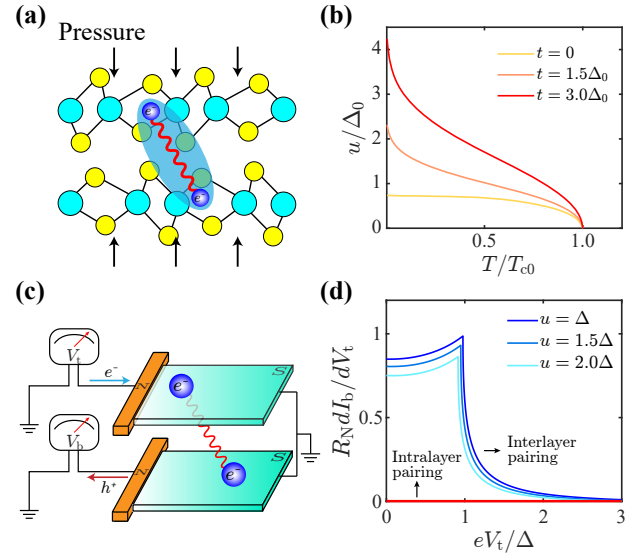


FIG. 3: Experimental implications of the interlayer pairing in a superconducting bilayer. (a) Schematics of the pressure-induced enhancement of the interlayer coupling, which further stabilizes the interlayer pairing. (b) The enhancement of the critical electrostatic potential energy u_c with increasing the interlayer coupling t . (c) Schematic illustration of the interlayer crossed Andreev reflection at the normal metal-superconducting bilayer interface. Since an incoming electron in the top layer is reflected as a hole in the bottom layer, the voltage drop in the bottom electrode is along the same direction as that in the electron-injecting top electrode. (d) The interlayer differential conductance spectra obtained from the bilayer BTK model. The differential conductance is normalized by the local resistance R_N of the normal junction. The conductance dI_b/dV_t decreases with increasing u due to the suppression of interlayer pairing, and vanishes entirely in the case of intralayer pairing. Here, $V_{t(b)}$ and $I_{t(b)}$ denote the voltage and current measured in the top (bottom) electrodes, respectively. In the simulation, we take $Z = 0.2$ and $t = 4.5\Delta$.

reversal, consistent with the experimental observation in bilayer T_d -MoTe₂ [31]. We note that while our simulated hysteresis curves are perfectly symmetric, experimental observations may show asymmetric characteristics due to extrinsic device asymmetries [31].

Implications of interlayer pairing.— In a superconducting bilayer, we have established interlayer pairing as the origin of the ferroelectric hysteretic switching of superconductivity. This naturally raises the question of how to experimentally verify our interlayer pairing scenario. The path to experimental verification lies in characterizing the physical consequences of interlayer pairing in the superconducting bilayer.

A key consequence of interlayer pairing is that the upper critical displacement field is enhanced with stronger interlayer coupling, as shown in Fig. 3(a) and (b). The Landau Ginzburg free energy density in Eq. 6 demonstrates the enhancement of u_c explicitly: the interlayer coupling t effectively reduces the depairing effect of u ,

thereby enhancing u_c in a manner analogous to the enhancement of paramagnetic limiting field via Ising spin-orbit coupling in Ising superconductors [43–47]. Experimentally, it has been reported that applying pressure to a bilayer system can enhance the interlayer coupling [48, 49]. Therefore, measuring the evolution of the superconducting region in the displacement field-temperature diagram under pressure serves as a direct test of the interlayer pairing scenario.

Another key signature of interlayer pairing is the interlayer crossed Andreev reflection as illustrated in Fig. 3(c) and (d). At the metal-superconducting bilayer interface, the interlayer pairing enables a crossed Andreev reflection that converts an incident electron in the top layer to a backward hole in the bottom layer. The occurrence of interlayer crossed Andreev reflection can be detected by measuring the voltage across the normal electrode contacting the bottom layer: the left moving holes in the bottom electrode generate a voltage drop in the same direction as that in the electron-injecting top electrode, while in the normal regime ($T > T_c$) the voltage drops in the two electrodes are oppositely directed [50–52]. Crucially, our simulations of the bilayer BTK model [42, 53] show that the interlayer crossed Andreev reflection exhibits gate-tunable behavior: increasing u slightly suppresses the interlayer crossed Andreev reflection while enhancing the local intralayer Andreev reflection (see Fig. 3(d) and Fig. S3), consistent with our previous analysis regarding the suppressive effect of u on interlayer pairing. This gate-tunable interlayer crossed Andreev reflection, originating from interlayer pairing, is fundamentally distinct from the intralayer pairing induced local Andreev reflection [42]. As a nonlocal transport phenomenon, the interlayer crossed Andreev reflection can be detected through a combination of local and non-local conductance spectroscopies [52, 54, 55], which provides a clear experimental pathway to verify the interlayer pairing scenario.

Discussions.— In this work, we have developed a theoretical framework based on the interlayer pairing scenario to explain the mechanism behind the ferroelectric hysteretic switching of superconductivity in bilayer systems. As our theory remains phenomenological, one future challenge is to integrate the interlayer pairing scenario with the microscopic mechanism of sliding ferroelectricity [4–7]. The case of T_d -MoTe₂ is particularly instructive: superconductivity in the ferroelectric bilayer emerges only when both electron and hole pockets are present, with $T_c = 2.3$ K [31, 32], in sharp contrast to the monolayer where superconductivity exists in both the electron and hole dominated regime with an enhanced $T_c = 7$ K [56, 57]. This stark difference highlights a distinct superconducting mechanism in the ferroelectric bilayer. Given that structural fluctuations in bilayer ferroelectrics have been proposed to mediate the attractive pairing interactions [58], an interesting future direction is to further investigate the microscopic origin of electronic

interactions that specifically favor interlayer pairing.

Our theory establishes a paradigm for coupled ferroelectricity and superconductivity, rooted in the interplay between non-local interlayer pairing and a layer-polarized charge distribution. This framework is generalizable to other ferroelectric superconductors with more complex spatial structures [59–63] by considering the coupling of non-local pairing to their specific charge polarization profiles. Apart from our non-local interlayer pairing scenario, the electron shear phonon coupling in sliding ferroelectrics may also induce the critical competition between ferroelectric order and superconductivity [58]. Crucially, our theory identifies two fundamental criteria governing the ferroelectric-superconducting coupling: the coexistence of ferroelectricity and superconductivity requires $P_r < P_c$, while ferroelectric hysteretic control of superconductivity is enabled by $P_c < P_s$. Intriguingly, the recent observation of orbital magnetic hysteresis persisting into the superconducting states in rhombohedral graphene [64] and twisted bilayer MoTe₂ [65] exhibits a formal similarity to the ferroelectric hysteresis studied here. Consequently, our phenomenological theory of ferroelectric-superconducting coupling may provide a basic paradigm for understanding the coupling between orbital magnetism and superconductivity in these systems, which are promising candidates for hosting chiral superconductivity.

Acknowledgements.— W.-Y.H. acknowledges the support from the National Natural Science Foundation of China (No. 12304200), the BHYJRC Program from the Ministry of Education of China (No. SPST-RC-10), the Shanghai Rising-Star Program (24QA2705400), and the start-up funding from ShanghaiTech University.

* These authors contributed equally to this work

† hewy@shanghaitech.edu.cn

- [1] K. Uchino, *Ferroelectric Devices* (CRC Press, 2009).
- [2] L. W. Martin and A. M. Rappe, *Nat. Rev. Mater.* **2**, 16087 (2016).
- [3] A. I. Khan, A. Keshavarzi, and S. Datta, *Nat. Electron.* **3**, 588 (2017).
- [4] M. Wu and J. Li, *Proc. Natl. Acad. Sci. U. S. A.* **118**, e2115703118 (2021).
- [5] L. Li and M. Wu, *ACS Nano* **11**, 6382 (2017).
- [6] B. T. Zhou, V. Pathak, and M. Franz, *Phys. Rev. Lett.* **132**, 196801 (2024).
- [7] P. Tang and G. E. W. Bauer, *Phys. Rev. Lett.* **130**, 176801 (2023).
- [8] J. Li, G. Yu, C. Xu, and H. J. Xiang, *Phys. Rev. Lett.* **130**, 146801 (2023).
- [9] E. Y. Tsymbal, *Science* **372**, 1389 (2021).
- [10] C. Wang, L. You, D. Cobden and J. Wang, *Nat. Mater.* **22**, 542 (2023).
- [11] D. Zhang, P. Schoenherr, P. Sharma, and J. Seidel, *Nat. Rev. Mater.* **8**, 25 (2023).
- [12] P. Sharma, F.-X. Xiang, D.-F. Shao, D. Zhang, E. Y.

- Tsymbal, A. R. Hamilton, and J. Seidel, *Sci. Adv.* **5**, eaax5080 (2019).
- [13] S. Yuan, X. Luo, H. L. Chan, C. Xiao, Y. Dai, M. Xie, and J. Hao, *Nat. Commun.* **10**, 1775 (2019).
- [14] Y. Wan, T. Hu, X. Mao, J. Fu, K. Yuan, Y. Song, X. Gan, X. Xu, M. Zhu et al., *Phys. Rev. Lett.* **128**, 067601 (2022).
- [15] M. Vizner Stern, Y. Waschitz, W. Cao, I. Nevo, K. Watanabe, T. Taniguchi, E. Sela, M. Urbakh, O. Hod, and M. Ben Shalom, *Science* **372**, 1462 (2021).
- [16] Z. Fei, W. Zhao, T. A. Palomaki, B. Sun, M. K. Miller, Z. Zhao, J. Yan, X. Xu, and D. H. Cobden, *Nature* **560**, 336 (2018).
- [17] Z. Zheng, Q. Ma, Z. Bi et al., *Nature* **588**, 71 (2020).
- [18] K. Yasuda, X. Wang, K. Watanabe, T. Taniguchi, and P. Jarillo-Herrero, *Science* **372**, 1458 (2021).
- [19] S. C. de la Barrera, Q. Cao, Y. Gao, Y. Gao, V. S. Bheemarasetty, J. Yan, D. G. Mandrus, W. Zhu, D. Xiao, and B. M. Hunt, *Nat. Commun.* **12**, 5298 (2021).
- [20] X. Wang, K. Yasuda, Y. Zhang, S. Liu, K. Watanabe, T. Taniguchi, J. Hone, L. Fu, and P. Jarillo-Herrero, *Nat. Nanotechnol.* **17**, 161 (2022).
- [21] R. Niu, Z. Li, X. Han, Z. Qu, D. Ding, Z. Wang et al., *Nat. Commun.* **13**, 6241 (2022).
- [22] A. Weston, E. G. Castanon, V. Enaldiev et al., *Nat. Nanotechnol.* **17**, 390 (2022).
- [23] P. Meng, Y. Wu, R. Bian, E. Pan, B. Dong, X. Zhao et al., *Nat. Commun.* **13**, 7696 (2022).
- [24] F. Sui, M. Jin, Y. Zhang, R. Qi, Y.-N. Wu, R. Huang, F. Yue, and J. Chu, *Nat. Commun.* **14**, 36 (2023).
- [25] R. Bian, R. He, E. Pan, Z. Li et al., *Science* **385**, 57 (2024).
- [26] R. Niu, Z. Li, X. Han, Z. Qu, Q. Liu, Z. Wang et al., *Nat. Nanotechnol.* **20**, 346 (2025).
- [27] X. Li, B. Qin, Y. Wang, Y. Xi, Z. Huang, M. Zhao et al., *Nat. Commun.* **15**, 10921 (2024).
- [28] K. Yasuda, E. Z.-Geller, X. Wang, D. Bennett et al., *Science* **385**, 53 (2024).
- [29] L. Zhang, J. Ding, H. Xiang, N. Liu et al., *Nat. Commun.* **15**, 10905 (2024).
- [30] W. Li, X. Zhang, J. Yang, S. Zhou, C. Song, P. Cheng, Y.-Q. Zhang, B. Feng, Z. Wang, Y. Lu, K. Wu, and L. Chen, *Nat. Commun.* **14**, 2757 (2023).
- [31] A. Jindal, A. Saha, Z. Li, T. Taniguchi, K. Watanabe, J. C. Hone, T. Birol, R. M. Fernandes, C. R. Dean, A. N. Pasupathy, and D. A. Rhodes, *Nature* **613**, 48 (2023).
- [32] Z. Li, A. Jindal, A. Strasser, Y. He, W. Zheng, D. Graf et al., *Phys. Rev. Lett.* **133**, 216002 (2024).
- [33] D. R. Klein, L.-Q. Xia, D. MacNeill, K. Watanabe, T. Taniguchi, and P. Jarillo-Herrero, *Nat. Nanotechnol.* **18**, 331 (2023).
- [34] K. M. Rabe, M. Dawber, C. Lichtensteiger, C. H. Ahn, and J.-M. Triscone, Modern physics of ferroelectrics: Essential background, *Top. Appl. Phys.* **105**, 1 (2007).
- [35] P. Chandra and P. L. Littlewood, *Top. Appl. Phys.* **105**, 69 (2007).
- [36] K. Yasuda, *Nature* **613**, 33 (2023).
- [37] W. X. Zhou and A. Ariando, *Jpn. J. Appl. Phys.* **59**, SI0802 (2020).
- [38] J. Chen, P. Cui, and Z. Zhang, *Adv. Funct. Mater.* **34**, 2408625 (2024).
- [39] M. Ye. Zhuravlev, R. F. Sabirianov, S. S. Jaswal, and E. Y. Tsymbal, *Phys. Rev. Lett.* **94**, 246802 (2009).
- [40] A. M. Clogston, *Phys. Rev. Lett.* **9**, 266 (1962).
- [41] B. S. Chandrasekhar, *Appl. Phys. Lett.* **1**, 7 (1962).
- [42] See the Supplemental Materials for details on 1) mean field calculation of the u - T phase diagram for the superconducting bilayer; 2) the derivation of the out-of-plane electric polarization; 3) the derivation of electrostatic susceptibility; 4) the derivation of phenomenological Landau Ginzburg free energy; 5) BTK model for the Andreev reflection in a superconducting bilayer.
- [43] J. M. Lu, O. Zheliuk, I. Leermakers, N. Q. Yuan, U. Zeitler, K. T. Law, and J. T. Ye, *Science* **350**, 1353 (2015).
- [44] X. Xi, Z. Wang, W. Zhao, J.-H. Park, K. T. Law, H. Berger, L. Forró, J. Shan, K. F. Mak, *Nat. Phys.* **12**, 139 (2016).
- [45] Y. Saito, Y. Nakamura, M. S. Bahramy, Y. Kohama, J. Ye et al., *Nat. Phys.* **12**, 144 (2016).
- [46] S. C. Barrera, M. R. Sinko, D. P. Gopalan, N. Sivadas, K. L. Seyler et al., *Nat. Commun.* **9**, 1427 (2018).
- [47] E. Sohn, X. Xi, W.-Y. He, S. Jiang, Z. Wang et al., *Nat. Mater.* **17**, 504 (2018).
- [48] G. Du, L. Zhao, S. Li, J. Huang and S. Fang et al., *Nat. Commun.* **16**, 4901 (2025).
- [49] X. Xie, J. Chen, S. Li, J. Ding, J. He, Z. Liu, J.-T. Wang, and Y. Liu, *Nano Letters*, **25**, 8571 (2025).
- [50] S. Russo, M. Kroug, T. M. Klapwijk, and A. F. Morpurgo, *Phys. Rev. Lett.* **95**, 027002 (2005).
- [51] A. Bordin, G. Wang, C.-X. Liu et al., *Phys. Rev. X* **13**, 031031 (2023).
- [52] J. Feng, H. F. Legg, M. Bagchi, D. Loss, J. Klinovaja, and Y. Ando, *Nat. Phys.* **21**, 708 (2025).
- [53] M. Tinkham, *Introduction to Superconductivity* (Dover Publications, New York, 2004).
- [54] J. Gramich, A. Baumgartner, and C. Schönenberger, *Phys. Rev. B* **96**, 195418 (2017).
- [55] J. Fuchs, M. Barth, C. Gorini, Í. Adagideli, and K. Richter, *Phys. Rev. B* **104**, 085415 (2021).
- [56] D. A. Rhodes, A. Jindal, N. F. Q. Yuan, Y. Jung et al., *Nano Lett.* **21**, 2505 (2021).
- [57] F. Tang, P. Wang, Q. Wang, Y. Gan, J. Lyu, X. Mi, M. He, L. Zhang, and J. H. Smet, *Nano. Lett.* **23**, 7516 (2023).
- [58] G. Chaudhary and I. Martin, *Phys. Rev. Lett.* **133**, 246001 (2024).
- [59] X. Yu, W. Zhong, S. Kawaguchi, H. Kadobayashi, X. Wang et al., *arXiv: 2410.22823*
- [60] M. Zhang, M. Qin, Y. Sun, S. Hong, and Y. Xie, *arXiv: 2506.16298*
- [61] J. Chen, W.-Y. Tong, P. Cui, and Z. Zhang, *arXiv: 2409.19265*.
- [62] J. Chen, W. Qin, P. Cui, and Z. Zhang, *Phys. Rev. B* **108**, L060501 (2023).
- [63] C. Enderlein, J. F. de Oliveira, D. A. Tompsett, E. B. Saitovitch, S. S. Saxena, G. G. Lonzarich, and S. E. Rowley, *Nat. Commun.* **11**, 4852 (2020).
- [64] T. Han, Z. Lu, Z. Hadjri, L. Shi, Z. Wu, W. Xu, Y. Yao et al., *Nature* **643**, 654 (2025).
- [65] F. Xu, Z. Sun, J. Li, C. Zheng, C. Xu, J. Gao, T. Jia et al., *arXiv: 2504.06972*